



ELSEVIER

Organic Electronics 3 (2002) 93–103

**Organic
Electronics**

www.elsevier.com/locate/orgel

AC measurements on binary phthalocyanine films

G.L. Pakhomov^{a,*}, V.I. Shashkin^a, D.E. Pozdnyaev^b, C. Muller^c, J.-M. Ribo^c^a *Institute for Physics of Microstructures, Russian Academy of Sciences, Russian Federation, GSP-105, 603950 Nizhny Novgorod, Russia*^b *All-Russian Research Institute for Experimental Physics, 607190, Sarov, Russia*^c *Universitat de Barcelona, Marti i Franques 1, E-08028 Barcelona, Spain*

Received 30 January 2002; accepted 3 July 2002

Abstract

The impedance spectra of thin films composed of lead phthalocyanine and vanadyl phthalocyanine in various proportions were studied over a large range of frequencies. The experimental data were simulated with a serial RC network consisting of three terms. The behavior of each term was analyzed as a function of film composition and ambient atmosphere. The applicability of known models has been evaluated.

© 2002 Elsevier Science B.V. All rights reserved.

PACS: 84.37.+q; 73.61.Ph

Keywords: Phthalocyanines; Thin films; Doping; Impedance spectroscopy

1. Introduction

Lead phthalocyanine (PcPb) is one of the most widely studied porphyrin type compounds proposed for use in organic electronics [1,2]. In particular, polycrystalline films based on PcPb have acquired great importance in chemical sensors using a sensitive element operating in an electrical mode [3]. The target gases used for testing are usually nitrogen oxides. Vapor-deposited PcPb layers have a relatively high initial conductivity, a detectable response towards NO_x concentration down to the ppb level [3–6]; their structure and electric properties are well-known [1–9]. Yet, full

range impedance spectra (IS) of PcPb thin films covering both high frequency (HF) and low frequency (LF) bands are obviously missing in published articles [1,5,10–16, and references therein].

PcPb molecules, as well as the molecules of oxometal phthalocyanines like PcTiO and PcVO, have a pyramidal shape and crystallize in similar crystal structures, which differ from the conventional (planar) transition metal complexes (PcMe) [7]. The predominating phase (monoclinic, triclinic or amorphous) is determined by such factors as substrate temperature and material, evaporation rate and annealing [4–6,8]. Based on the principle of geometric similarity [17], it is assumed that during physical vapor deposition (PVD) a mutual replacement of structurally similar molecules can take place in the growing crystals without changing the structure type [9,18,19]. Thus, in the case of PcMe(1) doped with another structurally related

* Corresponding author. Tel.: +7-8312-675535; fax: +7-8312-675553.

E-mail address: pakhomov@ipm.sci-nnov.ru (G.L. Pakhomov).

PcMe(2), no essential alteration in the molecular arrangement is expected, whereas the individual physical and chemical properties of the dopant molecules (e.g., their redox potentials) can be different and thus modify the electronic properties of the mixed crystal [2,9,16]. This is an advantage over the doping with more dissimilar inorganic or organic strong donor or acceptor molecules (e.g., metals, TCNQ, F-TCNQ, C₆₀), which do not form homogeneous mixed crystal with phthalocyanines, but, rather, lead to uncontrolled disordering. The latter systems are therefore more difficult to understand as there are too many factors that need to be examined.

Here, the results of AC conductivity measurements on PcPb thin films doped with vanadyl phthalocyanine (PcVO) are reported. An approach to the study of multi-component PcM films using DC and AC experiments was discussed earlier [12,20]. The measurements were performed both in air and in vacuum and aimed at establishing the influence of ambient atmosphere. Simple gas physisorption may modify electrical properties of the bulk PcMe material; therefore a comparison of the results obtained under well-controlled laboratory conditions (vacuum or inert gas atmosphere) with those taken under environmental conditions is a first step to evaluate the material properties for practical purposes [3]. Application of IS measurements with interdigital electrodes for oxidative gas detection was considered in [21], and in particular, employing phthalocyanine derivatives in [10]. Note, however, that most experiments so far have been done with sandwich-type devices fully covered by metal electrodes [1,11,14–16,22], which is not a suitable geometry for use as chemical gas sensors.

2. Experiment

Two-component PcPb/PcVO films were obtained by PVD in the vacuum equipment (VUP-5, SU) by batch operation. Various compositions were obtained by using co-deposition from two molecular beams with the *in situ* monitoring of the evaporation and the film deposition rates. The equipment and the experimental techniques have

been described elsewhere [12,20]. Films were made ≈ 200 nm thick; the substrate temperature did not exceed 313 K during deposition. The substrates consisted of a thin insulating support (polycrystalline Al₂O₃) with photolithographically made nickel electrode structures with an interelectrode gap of 100 μ m and an overall gap length between the 50 interdigital electrodes of 45 cm. Current versus voltage (J/V) plots of the device showed a linear dependence between -10 and $+10$ V.

The samples were then placed in a dark, shielded steel chamber filled with ambient air at room temperature and measured. After completion of the first series of instrumental sweeps in air, the chamber was pumped down to $<10^{-4}$ Pa, and after 2 h exposure to vacuum the measurements were repeated.

IS data in the range of 10^5 – 10^{-3} Hz were acquired with a frequency response analyzer (Schlumberger 1255) coupled to a potentiostat (EG&G PARC 273), both connected to a computer. The experimental points were recorded and analyzed in Bode ($|Z| = f(F[\text{Hz}])$, phase = $f(F[\text{Hz}])$) and in Nyquist ($Z'' = f(Z')$) coordinates, using the software *Z_View* 1.4d (Scribner), based on the program LEVM 6.0 written by Dr. J. Ross MacDonald [13].

3. Results

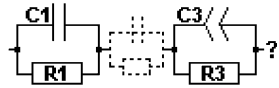
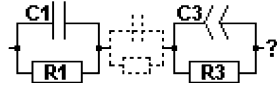
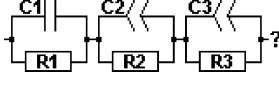
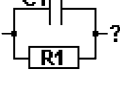
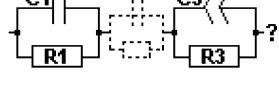
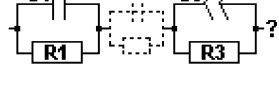
An overview over the seven composition ratios, measured in air and in vacuum, is given in Table 1.

For each composition, different probing AC voltages (50–200 mV) and DC bias potentials (0–3 V) were applied, cf. [14,15,23,24]. Since the samples are highly resistive, a superimposed voltage and/or elevated AC amplitudes were often necessary to acquire good quality data. Several sweeps with fixed regimes were performed on each sample in order to check the cyclic reproducibility.

Table 1
Table of compositions

Sample no.	I	II	III	IV	V	VI	VII
PcPb content, mol.%	100	83	66	50	29	17	0
PcVO content, mol.%	0	17	34	50	71	83	100

Table 2
Table of parameters

No.	Equivalent circuits	Parameters ^a								Comments
		R1 (MΩ)	C1 (pF)	ψ1	τ _{D1} (ms)	R3 (MΩ)	C3 (nF)	ψ3	τ _{D3} (s)	
<i>Vacuum</i>										
I		3.5 × 10 ¹ (2) ^b	45 (3)	0.98 (0.5)	1.3	5.2 (15)	10 (20)	0.81 (7)	2.5 × 10 ⁻²	The VLF “tile” with positive points, no DC dependence
II		6.1 (3)	46 (4)	0.98 (0.6)	0.29	1.2 (13)	15 (14)	0.72 (6)	5.0 × 10 ⁻²	The VLF “tile” with positive points, DC dependence—see Fig. 1
III ^c		9.6 (0.5)	43 (2)	0.98 (0.2)	0.40	1.8 (5)	46 (15)	0.96 (6)	7.4 × 10 ⁻²	Clear VLF “tile”, DC dependence for the 1st loop
IV		7.1 × 10 ¹ (0.2)	45 (1)	0.98 (0.2)	3.1	–	–	–	–	The VLF “tile” with positive points, DC dependence—see Fig. 2
V		1.2 × 10 ² (4)	44 (5)	0.99 (1)	5.3	4.5 × 10 ¹ (14)	4.9 (20)	0.8 (10)	1.5 × 10 ⁻¹	The VLF “tile”, DC dependence for the 1st loop
VI		7.0 × 10 ² (5)	34 (6)	1.0 (1)	23	2.3 × 10 ² (14)	0.78 (40)	0.89 (3)	1.3 × 10 ⁻¹	The VLF “tile” with positive points, strong DC dependence for the 1st loop
VII	unknown	> 3 × 10 ⁴	<1	–	–	–	–	–	–	No loops

(continued on next page)

Table 2 (continued)

No.	Equivalent circuits	Parameters ^a								Comments
		R1 (GΩ)	C1 (pF)	ψ1	τ _D 1 (ms)	R3 (GΩ)	C3 (nF)	ψ3	τ _D 3 (s)	
Air I		0.029 (5) ^b	57 (3)	0.99 (1)	1.5	0.073 (3)	2.2e-9 (7)	0.71 (1)	7.5 × 10 ⁻²	The VLF “tile”, DC dependence for the 1st loop
II ^c		0.010 (2)	40 (6)	1.0 (1)	0.4	0.006 (4)	1.2e-8 (10)	0.64 (3)	1.6 × 10 ⁻²	Little negative “tile”, DC dependence—see Fig. 1
III		0.052 (2)	40 (4)	0.99 (0.6)	2.1	0.019 (10)	8.4e-9 (19)	0.69 (6)	6.4 × 10 ⁻²	No “tile”, no DC dependence
IV		0.074 (0.5)	44 (3)	0.98 (0.3)	3.2	–	–	–	–	No “tile”, weak DC dependence
V		0.2 (3)	54 (2)	1.0 (1)	10	0.091 (15)	6.5e-9 (23)	0.78 (2)	5.0 × 10 ⁻¹	No “tile”, no DC dependence
VI		1.9 (4)	34 (3)	0.99 (0.4)	64	0.54 (14)	1.2e-9 (33)	0.9 (10)	6.0 × 10 ⁻¹	No “tile”, strong DC dependence for both 1st and 2nd loop
VII		28	27	–	–	–	–	–	–	The beginning of the semicircle

R and C are the equivalent resistance (Ω) and capacitance (F), τ_D is the average time constant/relaxation time (s), ψ is the fractional exponent, dimensionless,

is a common parallel RC combination, is a compound circuit (ZARC) with CPE (see, text), $Z_{cpe} = (j\omega\tau_D)^{-\psi}$ and $Z_{zarc} = R3/(1 + R3C3(j\omega)^\psi)$

[13], is the circuitual element whose parameters cannot be sufficiently fixed, ?—an additional VLF process.

^a AC amplitude—150 mV, DC bias—1.5 V.

^b In parentheses—the relative error, %.

^c 66% PcPb, vacuum: the parameters of the intermediate element: R2 = 2.5 MΩ (4.5%), C2 = 5.9 nF (21%), ψ2 = 0.82 (5.7%); 83% PcPb, air: R2 = 3.8 MΩ (3.7%), C2 = 9.2 nF (10%), ψ2—0.71 (1.6%), see text.

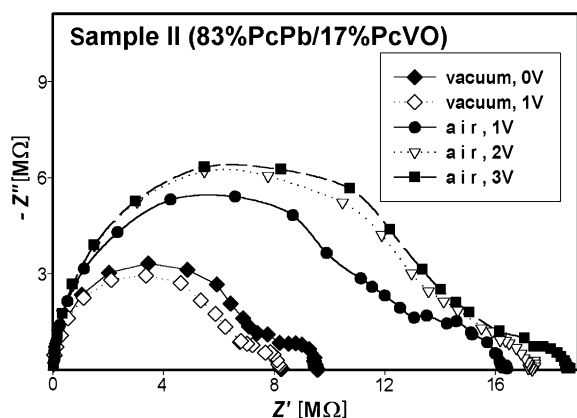


Fig. 1. Nyquist plot of the complex impedance for sample II in air (upper three curves) and in vacuum (lower two curves). The curves in vacuum and the curves in air correspond to different bias potentials (1, 0 V and 1, 2, 3 V, bottom to top, respectively).

The data of representative samples out of larger amount of measured samples are considered here.

The basic IS parameters are summarized in Table 2. Experimental curves on the complex plane (Nyquist plot) are presented in Fig. 1 for sample II, and in Fig. 2 for sample IV. The data for sample VII are omitted because of the extremely low conductance of the neat PcVO film, which gave a purely capacitive response in vacuum. Only the beginning of a Cole–Cole arc (non-ideal capacitor) was detected in air, accompanied by a noisy LF region.

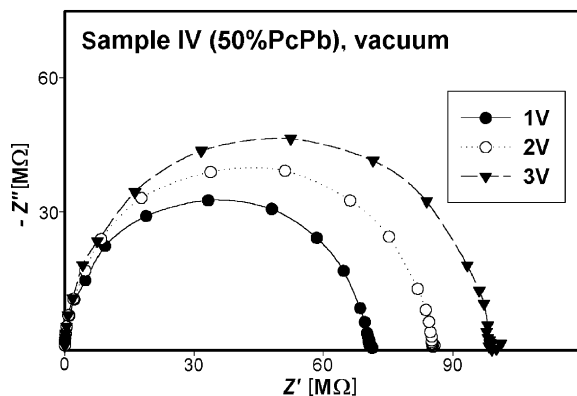


Fig. 2. Nyquist plot for sample IV measured in vacuum at different bias potentials (1, 2 and 3 V, bottom to top).

On the Nyquist plot two diffuse loops are seen for the samples I, II, III, V and VI (Fig. 1). The right part of the HF (first) semicircle and the left part of the LF (last) semicircle are distorted by an intermediate element. The calculated parameters are shown in Table 2, along with the respective equivalent scheme, that best fits the experimental data. The parameters of the intermediate element (second semicircle) are accessible only for sample II in air and for III in vacuum (Table 2, footnotes); in other cases they cannot be calculated precisely. The presence of this intermediate term is concluded from the line shapes and deviations in the numerical fitting results. Consequently, the error values for the LF semicircle parameters are greater (Table 2). The last points of the graphs (Figs. 1 and 2) may form a “tile” (U-shaped), which suggests additional processes in the very low frequency (VLF) region, <50 mHz, e.g., diffusion [15,25]. This effect is mainly displayed in the measurements carried out in vacuum (Table 2). Although at low frequencies the intergrain contacts dominate, problems caused by the electrode/layer interface, typical of two-terminal measurements, cannot completely be excluded [24]. Surprisingly, measurements in air yielded smooth data; contrary to this, the results obtained in vacuum were more scattered. Perhaps, there are distortions caused by the gas desorption from the interfacial areas of samples measured in the pumped chamber.

4. Discussion

Certain physical notions like the Havriliak–Negami [26], the Goswami–Goswami models [27], or the Jonscher response [23] can be invoked for interpretation of the IS data obtained from the PcMe samples, depending on the experimental conditions (mainly the temperature and frequency range) and the goal aimed at in these papers [1,5,10,11]. These notions focus basically on the HF domain, where the theory is well developed, and describe the dependence of the system admittance Y , or impedance Z , on the angular frequency $\omega = 2\pi F$ [1]. In the present investigation we are not so much interested in a general discussion, but,

rather, in an elaboration of a simple phenomenological scheme in order to characterize further the binary PcM films as gas sensor elements.

4.1. Simulation

Samples I, II, III, V and VI can be adequately simulated with a serial RC pair combination composed of three elements (Table 2). Adaptation of a single RC network, even upgraded with serial/parallel R or C [1,16,27], is obviously not adequate over a wide frequency range due to the resulting huge fitting errors. Analogous circuits were proposed for planar Met/PcMe/Met devices [14,15]. An accurate interpretation of each unit is nevertheless a difficult task. One of the reasons is the complex structure of the polycrystalline PcMe films. As known, frequency-dependent measurements simultaneously yield information about the grain interior, the grain boundaries and about electrode effects [10–16,23–25]. A serial combination of RC pairs was initially developed to parameterize solid state electrolytes with Maxwell–Wagner type conductivity [13,14,25]. Up to five terms could be resolved, including those related to gas absorption and diffusion [25]. Therefore, if the time constants are not different enough to allow visual separation, a thorough mathematical decomposition of overlapping arcs in IS is compulsory.

The first RC pair corresponds to an ideal situation, in which the semicircle center is placed on the real axis [13], i.e., ψ is very close or equal to unity (Table 2). The RC time constants (τ_D) are relatively large [11,15,16] and imply that we are probably dealing with secondary bulk processes. Primary bulk processes are expected to correspond to τ_D below 1 μ s (equivalent to the upper MHz region), which is beyond our experimental range. Indeed, variously shaped grains composing PcMe thin films [4,5] may contain smaller blocks (domains) with a monocrystalline structure, e.g., of the slipped stacks type [2,7], where a more efficient charge transport is observed [28]. High-resolution AFM images showing regular and disordered areas in the intragrain package for sublimed PcPb films, observed under vacuum [29], and most recently, for thin PcCu films, observed in air [30], have been published. In our experiments occa-

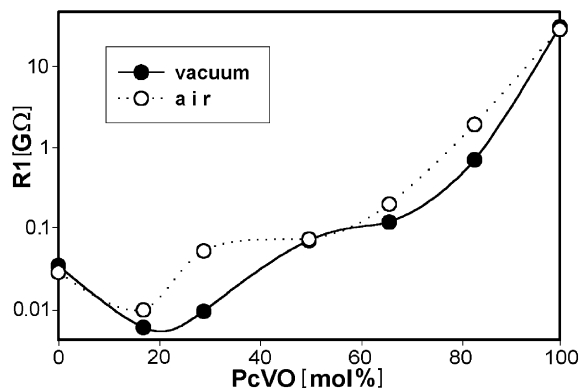


Fig. 3. The “composition-property” diagram for the equivalent resistance, R_1 (see text). 0% PcVO means 100% PcPb, i.e., sample I–Table 1.

sionally initial points, which may indicate a very HF semicircle, were registered. Another electrode pattern would be needed to be able to analyze such processes, as well as a more specialized instrumentation [24]. The C_1 capacitance is similar for all samples, while the R_1 resistance depends on the film composition (Table 2 and Fig. 3).

The third element produces semicircles having the center beneath the Z' -axis, i.e., depressed arc in impedance plane, ZARC [13] (Table 2). The displacement is stronger in air—Table 2. This points to an inhomogeneity in the process [11,13]. The equivalent capacitance parameter C_3 is approximately two orders of magnitude less than C_1 .

In both cases a deviation from ideal behavior was taken into account by using a constant phase element, CPE (Table 2, footnote). For the first semicircle this deviation is negligible, but introduction of a CPE is required for the third semicircle. Including the geometrical capacitance C_g [1,16,21] in parallel to the scheme or the leads resistance R_Ω preceding the scheme does not significantly modify the calculated parameters. In contrast to R_1 , the equivalent resistance R_3 depends on the atmosphere, rather, than on the film composition (Table 2).

4.2. Various compositions

For all samples, the “composition-property” diagrams are most suitable for a presentation of

experimental data. They are identical to those frequently used in physical chemistry for the analysis of binary systems. As PcMe have no melting point, other specific parameters (electrical, optical) can be used [17,18,31]. For one of the system properties, $R1$, such a diagram is presented in Fig. 3. The shape of these dependencies remains unaltered if τ_D (or any related) value is plotted on the Y-axis, instead of resistance.

Generally, when different components are mixed in a layer, a change of the bulk conductivity can be explained in terms of at least two contributions [22]. The first is a simple superposition of the individual conductivity properties. The conventional PcMe are p-type semiconductors [1,2], but their properties are dramatically affected by the preparation procedure and by the environment [3,8,28,35,36]. The introduction of one type of molecule in a foreign matrix could increase or decrease the overall conductivity. The mutual influences of the compounds and the definitive properties of the mixed polycrystalline film are difficult to predict.¹ The second contribution is a slight enhancement of structural disorder in the material caused by a non-ideal molecular isomorphism of mixed components. It may manifest itself through formation of additional point and planar defects typical for the PcMe microcrystals [29,30], antistructural defects and orientational disordering [17]. The induced structural stress, in turn, affects the charge transport, for instance, by the appearance of new traps [4]. An essential increase in the DC conductivity of the PcCu thin films has been observed after adding 10 wt.% PcVO [22], which was explained by a rise in the concentration

of defects in the mixed crystals serving as additional energetic traps (cf. Table 2).

Both curves in Fig. 3 depict almost monotonic alteration of the system property, in particular, of parameter $R1$. If the latter contribution (disordering) dominates, then a “crater-like” shape with a minimum $R1$ in the middle should be expected. In contrast, the evidence of the first leading contribution is shown (Fig. 3 and Table 2). Hence, a non-linear combination of the individual molecular properties mainly determines the bulk resistance of the layer. The relative influence of the components is different. For instance, adding 17% PcPb to the PcVO matrix decreases $R1$ 43 times, whereas adding the equivalent quantity of PcVO to the PcPb matrix decreases $R1$ 6 times (both in vacuum). On the whole, the minimal content of PcVO in the PcPb matrix causes maximal AC film conductance, whatever the atmosphere (Table 2, Fig. 3). DC measurements reveal the same phenomenon.

4.3. Evaluation of RC pairs

As mentioned above, each RC pair represents a semicircle on the Nyquist plot and is associated with a certain conductivity mechanism or condition. In [14] the HF semicircle was attributed to the bulk of PcM film, the interim semicircle to the space charge (SC) region and the LF semicircle to a highly resistive surface charge region. Another speculation was considered in [15]: the first semicircle was attributed to the hopping conductivity between and/or within crystals in the bulk material; the LF semicircles were ascribed to the band conduction within crystal or molecule. This reflects the prevalent opinion that the hopping model is more applicable for PcM at low temperatures and high frequencies, whereas the band model is useful at high temperatures and low frequencies [1,5,11,15,16]. Nevertheless, neither the former attribution (three regions), nor the latter attribution (two mechanisms) can be entirely carried over to the systems in question.

Obviously, the first element should comprise the bulk conduction within a grain. This is consistent with the sensitivity of the HF semicircle to the component ratio and with the corresponding τ_D

¹ The ionisation potentials (IP) may be used for a preliminary evaluation of the properties (e.g., electronic structure) of the mixed crystals [2,9,16,32]. In [9] energy levels of various PcMe in metal-free phthalocyanine solids have been investigated allowing for the difference in calculated IP values (4.97 eV for PcPb and 5.21 eV for PcAlX (PcVO not studied)). Solid state IP of PcVO measured by ultraviolet photo-emission spectroscopy is 5.3 eV [32], i.e., the difference in IP of PcPb and PcVO is relatively high [9]. The mutual influences of IP of various phthalocyanine derivatives on the properties of their layer-to-layer interfaces have been widely studied by Schlettwein et al. [35].

magnitudes (see also p. 4.4). A further separation, e.g., in inter- and intra-stack hopping contributions, appears to be impossible.

For all samples, any trial of quantitative understanding of the parameters of intermediate element can only be speculative. Presumably, the equivalent parameter R_2 is about one order of magnitude, the equivalent parameter C_2 —about two orders of magnitude less than in the first element (Table 2). Both values have an apparent trend to increase with the PcVO content. The intermediate circuit in a three-component scheme has been assigned to an extended SC region in the Schottky diodes, formed upon sandwiching a PcMe layer between an “ohmic” (Au, Zn, Ni) and a rectifying (In, Al) electrode [14]. However, this is not adequate for our devices as only symmetrical Ni electrodes were used, and we operated far below SC potentials (see Section 2). Moreover, the intermediate element did not vanish at zero voltage (Fig. 1).

The last LF semicircle should be associated with grain boundaries. First, the contribution of the intergrain contacts to the conductivity of these materials at lower frequencies has been highlighted repeatedly in various publications [1,11–16,21]. Recently, such a contribution has been derived from AC measurements on thin film polypyrrole sensors [24]. Second, the higher sensitivity of the LF semicircle to exposure to the atmosphere (Table 2) may be reasonably explained by a change in the gas adsorption across the grain surfaces, resulting in a change of the grain-to-grain impedance [28]. The likely candidates are molecular oxygen and water [1–3,14,28,35].

The third argument is connected with the IS data for sample IV—Fig. 2. The equimolar composition is an exceptional case, as shown in Fig. 2 and Table 2, where only one symmetrical loop was detected. According to the classification [7], both PcPb and PcVO molecules belong to the same type of molecular structure (type II). Taking into account the lattice parameters [7], the formation of a solid solution by the substitution principle may be assumed. Formation of solid solutions has been established by means of the X-ray diffraction for the PcCu/Cl₁₆ PcCu [31] and PcCu/PcVO [19] two-component films (see also [36]). Again, since the

components are not fully isomorphous (at least, the gravity centers of the molecules are different), the highest stress in the material should occur for the equimolar mixture. This will apparently prevent the growth of larger mixed crystallites [22] in the middle of the binary phase diagram. For amorphous PcPb films, the film surface is almost planar (smooth) and consists of well-resolved fine particles of 1.2 nm in the *Z*-direction [4]. So, we assume that for sample IV the intergrain conductivity cannot be separated from the intragrain one, the respective relaxation times merge, therefore, only one HF semicircle is found on the complex plane.² More details on the structural data will be published elsewhere.

4.4. Influence of DC and AC amplitudes

Most of the samples displayed a dependence of the HF loop on the bias potential (Figs. 1 and 2). The bulk conductivity of a PcMe film has been recognized to be bias independent [15] (if Schottky barriers are absent [23]). The DC dependence of the first loop on the Nyquist plot may originate from an active intermediate element in the proposed scheme. Indeed, the rise of Z'' in the middle frequency range is more pronounced for samples where the existence of an intermediate regime was already obvious (Fig. 1). Forward and reverse bias dependencies in the same frequency range have been reported in [14]. For sample IV (50% PcPb) this dependence exists, too (Fig. 2). Most probably, the bias dependent semicircle is placed directly under (or in place of) the first semicircle thus leading to an increase of its amplitude.

So, in the HF region (or more precisely in the HF and middle frequency regions), there are presumably two competitive mechanisms, e.g., two types of hopping, one of them being electrical field dependent. Unfortunately, there is no clear evi-

² Here, it is interesting to recall the Jonscher's remark: “We suggest that intermolecular hopping, especially between large molecules (PcMe), is indistinguishable from the Maxwell–Wagner mechanism with very small particle sizes and the extent of its applicability in molecular solids should be further investigated on controlled specimens of well-defined structure” [34].

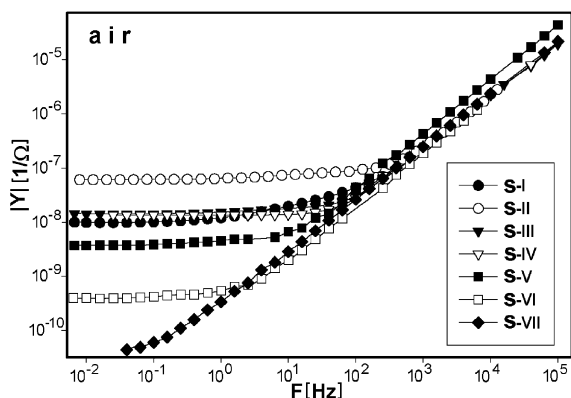


Fig. 4. The frequency dependence of the modulus of the admittance $|Y|$ for all samples in air. For clarity, the LF noise and error points are omitted.

dence whether the samples experienced the DC induced changes in air rather than in vacuum, thus not allowing to suggest an influence of oxygen [14,35].

A general graph of the frequency dependence of the modulus of the admittance for the samples in air is shown in Fig. 4. The HF section of each curve is linear; correlation coefficients are equal to 0.996 or better. The tangent of the slope for respective straight lines in the log–log scale lies in the range of 0.90–1.00, which is unambiguously associated with hopping conductivity in PcMe films [1,5,11,16,23,33,34]. The LF section tends asymptotically to constant admittance values (Fig. 4). The transition point shifts to the lower frequencies with an increase of the impedance, which is, in turn, proportional to $R1$ (Fig. 3). Such typical profiles of the function $|Y| = f(F[\text{Hz}])$ have been observed when measured at different temperatures [11,16]. In the present case, analogous profiles were obtained at constant room temperature by varying the film composition.

In Fig. 5 a typical dependence of the dissipation factor, $\tan\delta$, on the frequency is shown for the PcPb film. A monotonic line without an extremum proves that “ohmic” behavior is common for the electrodes used [14]. In the HF region $\tan\delta$ was found to decrease approximately as $1/\omega$, which is consistent with the Goswami and Goswami model [27] (see also [5,11,33]). The minimum of the dissipation factor, i.e., the region of dominating ω

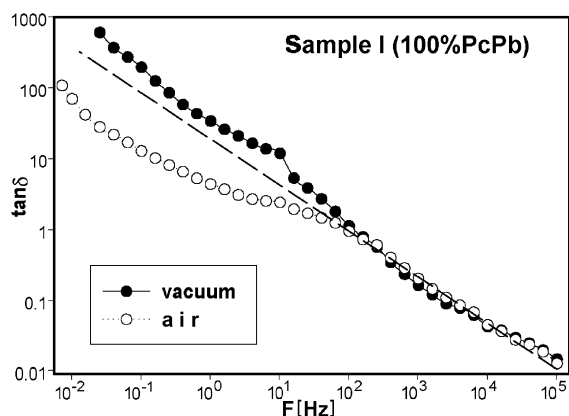


Fig. 5. The frequency dependence of the dissipation factor, $\tan\delta$, for sample I in air and in vacuum. The dashed line is a linear regression plotted for the data of the HF region.

term, was not reached in our experiments [33]. An extrapolation of the linear regression from the HF part (dashed line) reveals some distortions in the LF region (<10 Hz), which imply a spectrum of relaxation times (Fig. 5). In the VLF region $\tan\delta$ appears to be proportional to $(\omega)^{-1/2}$ in air, and to $(\omega)^{-3/4}$ in vacuum.

An increasing DC current usually provoked a rise in the noise amplitude. In the RC network the equivalent resistance $R1$ (or $R2$) increased (Figs. 1 and 2). The $C1$ capacitance was little affected. Both $R3$ and $C3$ values changed slightly. Increasing the AC amplitude led to an improvement of the signal-to-noise ratio [24], and in several cases semicircles in the LF range became more distinguishable. On the other hand, one has to be careful, because using higher AC amplitudes may result in distortions by non-linear effects [13].

5. Conclusions

A comparative study of the AC conductivity of thin films of binary mixtures of metal phthalocyanine molecular semiconductors provides useful information for fundamental and for application-oriented research [12,20,22,31]. An interesting superposition of individual molecular properties and structural properties of polycrystalline material has been found. Although the conceptions discussed

are somewhat oversimplified, which is inevitable when developing a generalized model for impedance spectroscopy data, we can draw some conclusions and offer suggestions for the further development of PcMe sensors:

- (i) Both AC and DC [20,31] conduction of a film composed of morphologically similar PcMe compounds can be significantly varied by changing the mixing ratio.
- (ii) The studied devices can be described with three-component equivalent circuit schemes, where the first element is mainly governed by the film composition, the second element by the bias potential, and the third element by the ambient atmosphere.
- (iii) The mutual influences of the components are not additive (Fig. 3).
- (iv) The LF band (10–0.1 Hz) is more sensitive to the atmosphere; it can be simulated with a self-dependent ZARC element in the equivalent circuit scheme.
- (v) Useful data are obtained for those instrumental setting ranges, where the lowest possible bias is combined with optimally high AC amplitude.

Acknowledgements

The authors wish to express their thanks to Profs. L.G. Pakhomov and A.E. Pochtenny for many helpful discussions. This work is supported by the RFBR Grant 00-02-16487. GLP acknowledges support by the INTAS Grant YSF 00-78.

References

- [1] R.D. Gould, *Coord. Chem. Rev.* 156 (1996) 237.
- [2] G. Guillaud, J. Simon, J.P. Germain, *Coord. Chem. Rev.* 178–180 (1998) 1433.
- [3] R. Zhou, F. Josse, W. Goepel, Z.Z. Ozturk, O. Bekaroglu, *Appl. Organomet. Chem.* 10 (1996) 557.
- [4] J.C. Hsieh, C.J. Liu, Y.H. Ju, *Thin Solid Films* 322 (1998) 98.
- [5] M.E. Azim-Araghi, D. Campbell, A. Krier, R.A. Collins, *Semicond. Sci. Technol.* 11 (1996) 39;
- [6] D. Campbell, R.A. Collins, *Phys. Stat. Sol. (a)* 152 (1995) 431.
- [7] C. Hamann, A. Mrwa, M. Muller, W. Goepel, M. Rager, *Sensors Actuators B* 4 (1991) 73.
- [8] M. Engel, Report Kawamura Inst. Chem. Res. 1997 (1996) 11.
- [9] H. Mockert, K. Graf, D. Schmeisser, W. Goepel, Z.A. Ahmad, P.B.M. Archer, A.V. Chadwick, J.D. Wright, *Sensors Actuators B* 2 (1990) 133.
- [10] R.O. Loutfy, Y.C. Cheng, *J. Chem. Phys.* 73 (1980) 2902.
- [11] J. Souto, M.L. Rodriguez-Mendez, J. de Saja-Gonzalez, J.A. de Saja, *Thin Solid Films* 284–285 (1996) 888.
- [12] A.S. Riad, M.T. Korayem, T.G. Abdel-Malik, *Phys. B* 270 (1999) 140.
- [13] G.L. Pakhomov, C. Muller, L.G. Pakhomov, D.E. Pozdnyaev, J.-M. Ribo, *Thin Solid Films* 304 (1997) 36.
- [14] J. Ross McDonald, *Impedance spectroscopy*, Wiley, New York, 1987.
- [15] B. Boudjema, G. Guillaud, M. Gamoudi, M. Maitrot, J.-J. Andre, M. Martin, J. Simon, *J. Appl. Phys.* 56 (1984) 2323.
- [16] R. Nowroozi-Esfahani, G.J. Maclay, *J. Appl. Phys.* 67 (1990) 3409.
- [17] O. El Beqqali, M. Al Sadoun, G. Guillaud, M. Gamoudi, M. Benkaddour, A.S. Skal, M. Maitrot, *J. Appl. Phys.* 69 (1991) 3670.
- [18] A.I. Kitaigorodski, *Molecular Crystals*, Nauka Publ., Moscow, 1971, Chapters 16,17; See also A.I. Kitaigorodski, *Mixed Crystals*, Nauka Publ., Moscow, 1983.
- [19] E.A. Lucia, F.D. Verderame, *J. Chem. Phys.* 48 (1968) 1835.
- [20] M. Starke, H. Wagner, C. Hamann, *Krist. und Techn.* B 7 (1972) 1319.
- [21] G.L. Pakhomov, Yu.D. Semchikov, L.G. Pakhomov, *Mendeleeev Comm.* (1995) 204.
- [22] H.-E. Endres, S. Drost, F. Hutter, *Sensors Actuators B* 22 (1994) 7.
- [23] C. Hamann, M. Starke, H. Wagner, *Phys. Stat. Sol. (a)* 16 (1973) 463.
- [24] A.K. Jonscher, *Thin Solid Films* 36 (1976) 1.
- [25] P.D. Harris, W.M. Arnold, M.K. Andrews, A.C. Partridge, *Sensors Actuators B* 42 (1997) 177.
- [26] C. Gabrielli, Identification of electrochemical processes by frequency response analysis, Technical report no. 004/83 of the Solartron Instruments Company, 1994.
- [27] S. Havriliak, S. Negami, *J. Polym. Sci. C* 14 (1966) 99.
- [28] A. Goswami, A.P. Goswami, *Thin Solid Films* 16 (1973) 175.
- [29] J.H. Schoen, Ch. Kloc, Zh. Bao, B. Batlogg, *Adv. Mater.* 12 (2000) 1539.
- [30] L. Ottaviano, L. Lozzi, A. Phani, A. Ciattoni, S. Santucci, S. Di Nardo, *Surf. Sci.* 136 (1998) 81.
- [31] R. Hiesgen, M. Raebisch, H. Boettcher, D. Meissner, *Sol. Energ. Mater. Sol. Cells* 61 (2000) 73.
- [32] D.E. Pozdnyaev, Ph.D. thesis, Lobachevsky State University, 1999, N. Novgorod, RF.

- [32] M. Pfeiffer, A. Beyer, T. Fritz, K. Leo, *Appl. Phys. Lett.* 73 (1998) 3202.
- [33] S.I. Shihub, R.D. Gould, S. Gravano, *Phys. B* 222 (1996) 136.
- [34] J.J. Fendley, A.K. Jonscher, *J. Chem. Soc. Farad. Trans.* 1 (69) (1973) 1213.
- [35] D. Schlettwein, K. Hesse, N.E. Gruhn, P.A. Lee, K.W. Nebesny, N.R. Armstrong, *J. Phys. Chem. B* 105 (2001) 4791; S. Hiller, D. Schlettwein, N.R. Armstrong, *D. Woehrl, J. Mater. Chem.* 8 (1998) 945.
- [36] T. Morioka, H. Tada, A. Koma, *J. Appl. Phys.* 73 (1993) 2207.